Deletion of GPI7, a yeast gene required for addition of a side chain to the glycosylphosphatidylinositol (GPI) core structure, affects GPI protein transport, remodeling, and cell wall integrity

Benachour, A; Sipos, G; Flury, I; Reggiori, Fulvio; Canivenc-Gansel, E; Vionnet, C; Conzelmann, A; Benghezal, M

Published in:
The Journal of Biological Chemistry

DOI:
10.1074/jbc.274.21.15251

THE JOURNAL OF BIOLOGICAL CHEMISTRY
Vol. 274, No. 21, Issue of May 21, pp. 15251–15261, 1999

Printed in U.S.A.

Deletion of *GPI7*, a Yeast Gene Required for Addition of a Side Chain to the Glycosylphosphatidylinositol (GPI) Core Structure, Affects GPI Protein Transport, Remodeling, and Cell Wall Integrity*

(Received for publication, January 26, 1999, and in revised form, March 1, 1999)

Abdellah Benachour‡, György Sipos§, Isabelle Flury, Fulvio Reggiori¶, Elisabeth Canivenc-Gansel, Christine Vionnet, Andreas Conzelmann‖, and Mohammed Benghezal**

From the Institute of Biochemistry, University of Fribourg, Chemin du Musée 5, CH-1700 Fribourg, Switzerland

***Gpi7* was isolated by screening for mutants defective in the surface expression of glycosylphosphatidylinositol (GPI) proteins. *Gpi7* mutants are deficient in YJL062w, herein named *GPI7*. *GPI7* is not essential, but its deletion renders cells hypersensitive to Calcofluor White, indicating cell wall fragility. Several aspects of GPI biosynthesis are disturbed in Δ*gpi7*. The extent of anchor remodeling, *i.e.* replacement of the primary lipid moiety of GPI anchors by ceramide, is significantly reduced, and the transport of GPI proteins to the Golgi is delayed. Gpi7p is a highly glycosylated integral membrane protein with 9–11 predicted transmembrane domains in the C-terminal part and a large, hydrophilic N-terminal ectodomain. The bulk of Gpi7p is located at the plasma membrane, but a small amount is found in the endoplasmic reticulum. *GPI7* has homologues in *Saccharomyces cerevisiae*, *Caenorhabditis elegans*, and man, but the precise biochemical function of this protein family is unknown. Based on the analysis of M4, an abnormal GPI lipid accumulating in *gpi7*, we propose that Gpi7p adds a side chain onto the GPI core structure. Indeed, when compared with complete GPI lipids, M4 lacks a previously unrecognized phosphodiester-linked side chain, possibly an ethanolamine phosphate. Gpi7p contains significant homology with phosphodiesterases suggesting that Gpi7p itself is the transferase adding a side chain to the α1,6-linked mannose of the GPI core structure.**

Glycosylphosphatidylinositol (GPI)[1]-anchored proteins represent a subclass of surface proteins found in virtually all eukaryotic organisms (1). The genome of *Saccharomyces cerevisiae* contains more than 70 open reading frames (ORFs) encoding for proteins that, as judged from the deduced primary sequence, can be predicted to be modified by the attachment of a GPI anchor (2, 3). In about 25 of them, the presence of an anchor has been confirmed biochemically. A majority of them lose part of the anchor and become covalently attached to the β1,6-glucans of the cell wall (4–6). A minority of GPI proteins retain the GPI anchor in an intact form and stay at the plasma membrane (PM).

For the biosynthesis of GPI anchors, phosphatidylinositol (PI) is modified by the stepwise addition of sugars and ethanolamine phosphate (EtN-P), thus forming a complete precursor lipid (CP) which subsequently is transferred *en bloc* by a transamidase onto newly synthesized proteins in the ER (7, 8). The identification of genes involved in the biosynthesis of the CP and its subsequent attachment to proteins has been possible through the complementation of mammalian and yeast gpi$^-$ mutants, *i.e.* mutants being deficient in GPI anchoring of membrane proteins (7, 9–20). In our laboratory, a series of recessive gpi$^-$ mutants (*gpi4* to *gpi10*) has been obtained by screening for yeast mutants that are unable to display the GPI-anchored α-agglutinin (Sag1p) at the outer surface of the cell wall, although the synthesis and secretion of soluble proteins is normal (21, 22).

Here we report on the characterization of *gpi7*. Four independent *gpi7* mutants accumulated M4, an abnormal GPI intermediate that is less hydrophilic than CP2, the precursor accumulating when the transfer of GPIs to proteins is interrupted (18, 19, 21, 23). Our preliminary characterization of M4 had shown that deacylation by NH_3 followed by HF treatment, used to hydrolyze selectively the phosphodiester bonds (Fig. 1), yielded the same Man_4-GlcN-inositol fragment as CP2, and we speculated that *gpi7* mutants may be unable to add the EtN-P onto Man3 (Fig. 1) (21). Here we show that this speculation was wrong, that CP2 differs from M4 with regard to a previously unrecognized side chain attached to Man2 (Fig. 1), and that *GPI7* is required for the attachment of this side chain.

EXPERIMENTAL PROCEDURES

Strains, Growth Conditions, and Materials—S. cerevisiae strains were FBY11 (*MAT***a** *ade2-1 ura3-1 leu2-3,112 trp1-1 his3-11,15 gpi8-1*), FBY15 (*MATα ade2-1 ura3-1 leu2-3,112 trp1-1 his3-11,15 gpi7-1*), W303-1B (*MATα ade2-1 can1-100 ura3-1 leu2-3, 112 trp1-1 his3-11,15*),

* This work was supported by Grant 3100-032515 from the Swiss National Foundation. The costs of publication of this article were defrayed in part by the payment of page charges. This article must therefore be hereby marked "*advertisement*" in accordance with 18 U.S.C. Section 1734 solely to indicate this fact.

‡ Present address: Université de Caen, IRBA, Laboratoire de Microbiologie de l'Environnement, Caen, France.

§ Present address: % R. S. Fuller, University of Michigan Medical Center, Dept. of Biological Chemistry, Ann Arbor, MI 48109-0606.

¶ Present address: % H. Pelham, MRC, Laboratory of Molecular Biology, Cambridge, UK.

‖ To whom correspondence should be addressed: Institute of Biochemistry, Chemin du Musée 5, CH-1700 Fribourg, Switzerland. Tel.: 41 26 300 8630; Fax: 41 26 300 9735: E-mail: andreas.conzelmann@unifr.ch.

** Present address: Plant Cell Biology, Research School of Biological Sciences, Australian National University, Canberra ACT 2601, Australia.

[1] The abbreviations used are: GPI, glycosylphosphatidylinositol; ASAM, *A. satoi* α-mannosidase; CP, complete precursor; DAG, diacylglycerol; DHS, dihydrosphingosine; EtN-P, ethanolamine phosphate; GPI-PLD, GPI-specific phospholipase D; Ins, *myo*-inositol; JBAM, jack bean α-mannosidase; Man, mannose; ORF, open reading frame; pC1 and pC2, protein-derived Ceramides 1 and 2; pG1 protein-derived Glycerophospholipid 1; PI, phosphatidylinositol; PM, plasma membrane; ts, thermosensitive; wt, wild type; PAGE, polyacrylamide gel electrophoresis; PIPES, 1,4-piperazinediethanesulfonic acid; nt, nucleotide; PCR, polymerase chain reaction; kb, kilobase pair(s); HPLC, high pressure liquid chromatography.

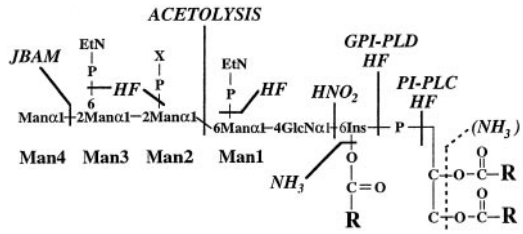

FIG. 1. **Presumed structure of the complete yeast precursor glycolipid CP2.** Relevant cleavage procedures are indicated. Man1, Man2, Man3, and Man4 designate the α1,4-linked, α1,6-linked, and α1,2-linked mannoses (Man). *X* indicates an HF-sensitive group that is not yet defined chemically. *R,* alkyl; *P,* phosphate.

X2180-1A (*MAT**a** lys*$^-$), FBY122 (MAT***a*** *ade2-1 ura3-1 leu2-3,112 trp1-1 his3-11,15 gpi8-1 gpi7-1*), FBY182 (*MATα ade2-1 ura3-1 leu2-3,112 his3-11,15 gpi7::KanMX4*), HMSF176 (*MAT**a** sec18-1*), FBY49 (*MAT**a** sec18-1 gpi7::KanMX4*), C4 (*MAT**a** ura3-52 leu2-3,112 pmi40*), HMSF331 (*MAT**a** sec53-6*), LB2134-3B (*MAT**a** mnn9*), and YNS3-7A (*MAT**a** ura3 his*$^-$ *mnn1 och1::LEU2*). Diploid strains were FBY118 (*MAT**a**/α ade2-1/ade2-1 ura3-1/ura3-1 leu2-3, 112/leu2-3,112 TRP1/trp1-1 his3-11,15/his3-11,15 LYS/lys*$^-$), FBY40 (MAT***a***/*α ade2-1/ade2-1 ura3-1/ura3-1 leu2-3,112/leu2-3,112 TRP1/trp1-1 his3-11,15/his3-11,15 LYS/lys*$^-$ *GPI7/gpi7-1*), and FBY43 (*MAT**a**/α ade2-1/ade2-1 ura3-1/ura3-1 leu2-3,112/leu2-3,112 TRP1/trp1-1 his3-11,15/his3-11,15 LYS/lys*$^-$ *gpi7::KanMX4/gpi7::KanMX4*). Maintenance and growth conditions have been described (19). The absorbance of dilute cell suspensions was measured in a 1-cm cuvette at 600 nm, and one A_{600} unit of cells corresponds to 1–2 $\times$ 10^7 cells depending on the strain. *Escherichia coli* strains were HB-101, XL1 blue, and M15 [pREP4] (Qiagen).

Materials were obtained from the sources described recently (22). Cysteamine was from Sigma; [^{3}H]dihydrosphingosine was synthesized as described (24); myriocin was a kind gift of Dr. N. Rao Movva (Novartis, Basel, Switzerland); antibodies to Och1p, alkaline phosphatase, Kex2p, and Wbp1p were kindly donated by Dr. Y. Jigami, National Institute of Bioscience and Human Technology, Ibaraki 305, Japan; Dr. S. Emr, Howard Hughes Medical Institute, University of California, San Diego; Dr. R. Fuller, University of Michigan Medical Center, Ann Arbor, MI; and Dr. M. Aebi, Mikrobiologisches Institut, ETH Zürich, Switzerland, respectively.

Cloning, Partial Sequencing, and Disruption of GPI7—The *GPI7* gene was cloned by complementation of the ts growth phenotype of the *gpi7-1/gpi8-1* double mutant as described (19). The three plasmids complementing *gpi7-1* contained a 4.3-kb common DNA restriction fragment that was partially sequenced by the dideoxy sequencing method (25). The complementing insert *Sph*I/*Ssp*I of 3.6 kb was cloned into the *Sph*I/*Sma*I-digested YEp352 multicopy vector (26) or YCplac33 single copy vector (27) to generate pBF41 (Fig. 3*C*) and pBF43, respectively.

One step disruption of *GPI7* was done as described (28). Briefly, the 1.5-kb long KanMX4 module was PCR-amplified by using pFA6a-KanMX4 as template and the following two adapter primers: GPI7-forwards (5′-CTTCACCAAGTTAGCAAG**ATG**AACTTGAAGCAGTTC-ACGTGCCTcgatgaattcgagctc-3′) with 17 nucleotides (nt) of homology to the pFA6a-KanMX4 multiple cloning site (in *lowercase*) and 43 nt of homology to *GPI7* (in uppercase) starting 18 nt upstream of the start codon (*bold*); GPI7-backwards (5′-ATCAAGAGCGCAAAGGAGGGCC-AATTCAGGTAACCAGCCATTCAcgtacgctgcaggtcgac-3′) with 18 nt of homology to the pFA6a-KanMX4 multiple cloning site (*lowercase*) and 44 nt of homology to the ORF of *GPI7* in the region immediately upstream of the stop codon. This PCR DNA fragment was used to transform the diploid strain FBY118, homozygous for *GPI7*, and FBY40, a heterozygous *gpi7-1/GPI7* strain. The correct targeting of the PCR-made KanMX4 module into the *GPI7* locus in geneticin-resistant clones was verified by PCR with whole yeast cells using primers GPI7-plus (5′-GTTCATCTACCACGCAC-3′) starting 36 nt upstream of the ATG, GPI7-minus (5′-GACCCAAGTAATGCAGG-3′) starting 631 base pairs downstream of the ATG and the K2 primer of the KanMX4 module (5′-GTATTGATGTTGGACG-3′).

Purification of Recombinant His-tagged Gpi7p and Antibody Production—Plasmid pBF41 (Fig. 3*C*) was digested with *Bst*YI and *Eco*RV to generate a 633-base pair fragment of *GPI7*. This fragment was inserted into the multiple cloning site of the bacterial expression vector pQE-30 (Qiagen) digested with *Bam*HI/*Sma*I thus generating the plasmid pBF402. This plasmid was used to transform the *E. coli* strain M15[pREP4]. Expression of the recombinant protein was induced with isopropyl-1-thio-β-D-galactopyranoside and purified on a nickel-nitrilotriacetic acid-agarose column (Qiagen) under denaturing conditions according to the manufacturer's instructions. A polyclonal antiserum was raised against this Gpi7p fragment by repeated intramuscular injections of 100 μg of recombinant protein into a rabbit. Ten mg of the recombinant protein were coupled to CNBr-activated Sepharose 4B (Amersham Pharmacia Biotech) according to the manufacturer's instructions, and antiserum was affinity purified as described (29).

Membrane Association, Protease Sensitivity, and Cellular Localization of Gpi7p—The nature of the association of Gpi7p with the membrane was determined following a previously described protocol (30) except that the EDTA concentration in buffer G was increased from 2 to 20 mM. Gpi7p protease sensitivity was examined by proteinase K digestion of microsomes essentially as described (31). Briefly, 100 A_{600} of washed W303 cells were resuspended in 1 ml of lysis buffer (20 mM HEPES, pH 7.5, 500 mM sucrose, 3 mM magnesium acetate, 20 mM EDTA, 1 mM dithiothreitol) and were lysed by agitation with glass beads at 4 °C. The homogenate was centrifuged for 5 min at 600 $\times$ *g* to remove unbroken cells, and the supernatant was centrifuged for 15 min at 13,000 $\times$ *g*. The membrane pellet was resuspended in 240 μl of the same lysis buffer and split into 6 aliquots of equal size. Aliquots of microsomes were incubated for 20 min on ice with or without 0.5% Triton X-100 and proteinase K. Digestions were stopped by addition of phenylmethylsulfonyl fluoride (final concentration 4 mM, added from a 200 mM stock in ethanol) and kept on ice for an additional 10 min before being boiled in sample buffer (32). The subcellular localization of Gpi7p was determined essentially as described (33). Briefly, 500 A_{600} units of mid-log phase W303-1B cells were broken by agitation with glass beads in 200 mM sorbitol, 25 mM PIPES, pH 6.8, 50 mM KCl, 5 mM NaCl, 10 mM EDTA, 10 mM NaN_3/NaF, 1 mM phenylmethylsulfonyl fluoride, leupeptin, pepstatin, and antipain, each at 30 μg/ml). After removal of the unbroken cells the homogenate was centrifuged for 10 min at 8,000 $\times$ *g* at 4 °C to generate pellet P8 and supernatant S8. S8 was divided in two and either precipitated by the addition of trichloroacetic acid to 10% or centrifuged at 100,000 $\times$ *g* for 1 h to generate pellet P100. For zymolyase treatment the cells were washed and resuspended at 50 A_{600} units/ml in zymolyase buffer (1.2 M sorbitol, 50 mM K_2HPO_4 pH 7.5, 40 mM 2-mercaptoethanol, 20 mM EDTA, 10 mM NaN_3, 10 mM NaF) containing zymolyase 20T. After a 40-min incubation at 30 °C, cells were placed on a cushion of 1.5 M sorbitol, 50 mM K_2HPO_4, pH 7.5, 20 mM EDTA, 10 mM NaN_3, 10 mM NaF and were centrifuged. For Western blotting, all the samples were denatured during 5 min at 95 °C in reducing sample buffer and run on a 6, 7.5, or 10% SDS-PAGE for detection of antigens, respectively (32). Western blotting was carried out with anti-Wbp1p, anti-alkaline phosphatase, anti-Gas1p, or anti-Kex2p antisera or with affinity purified anti-Gpi7p or anti-Och1p antibodies, always using the chemiluminescence ECL kit from Amersham Pharmacia Biotech, Buckinghamshire, UK.

Labeling of Cells—Previously described procedures were used to label cells with [2-^{3}H]Man (23), [4,5-^{3}H]DHS, or [2-^{3}H]Ins (24) and to label microsomes with UDP-[^{3}H]GlcNAc (22). Delipidated protein extracts for SDS-PAGE and lipid extracts were made as described (24). Lipid extracts were analyzed by ascending TLC using 0.2-mm thick silica gel 60 plates with the solvent 1 (chloroform/methanol, 0.25% KCl in water, 55:45:10, v/v) or solvent 2 (chloroform/methanol/water, 10:10:3, v/v). Radioactivity was detected and quantitated by one- and two-dimensional radioscanning (LB 2842; Berthold AG, Regensdorf, Switzerland). TLC plates were sprayed with EN^{3}HANCE and exposed to film (X-Omat; Eastman Kodak Co.) at −80 °C.

Analytical Methods—Lipid extracts were deacylated with NaOH (34) and treated with JBAM (35) as described. For GPI-PLD treatment lipid extracts were dissolved in 20 mM Tris-HCl, pH 7.4, 0.1 mM $CaCl_2$, 20% 1-propanol. Incubations were for 12 h at 37 °C. All treated lipid extracts were desalted by partitioning between *n*-butyl alcohol and an aqueous solution of 0.1 mM EDTA, 5 mM Tris-HCl, pH 7.5, and back extraction of the butanol phase with water before TLC (23). Lipids were treated with methanolic NH_3 to remove the acyl group on Ins (36) and cleaved using nitrous acid (37) as described. Lipids were purified by preparative TLC on 0.2-mm thick Silica Gel 60 plates (Merck, Germany) in solvent 2. Radioactive spots were localized by radioscanning, scraped, and eluted with solvent 2. A second run on TLC was done to obtain radiochemically pure M0, M4, and CP2.

Soluble head groups were obtained from lipids through GPI-PLD treatment done as above, followed by limiting methanolic NH_3 deacylation (36). Non-hydrolyzed GPIs were removed by butanol extraction (23). The water-soluble head groups were treated with JBAM (0.5 units) or ASAM (5 microunits) as described (38). HF dephosphorylation was

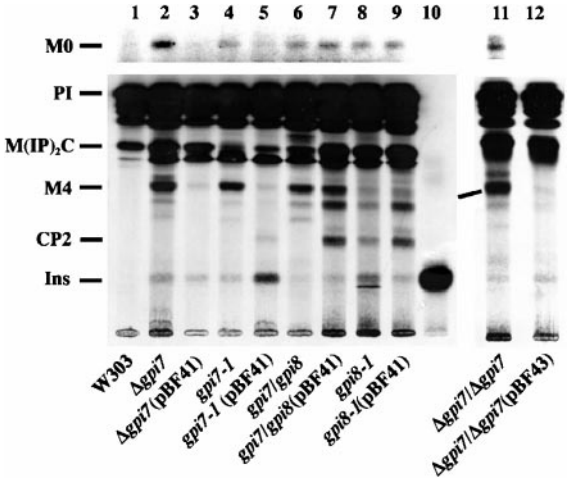

FIG. 2. **Complementation of *gpi7* mutants by YJL062w.** Exponentially growing cells were radiolabeled at 37 °C with [^{3}H]Ins (2 μCi/A_{600}), and desalted lipid extracts were analyzed by TLC (solvent 2) and fluorography. The same amount of radioactivity was spotted in each lane. *M(IP)$_2$C,* inositol phosphomannosylinositol phosphoceramide. The upper part of the fluorogram was scanned at higher sensitivity to bring into view the faint bands of *M0*. *Lane 10* contains [^{3}H]Ins. Samples still contain residual amounts of free [^{3}H]Ins after extraction into butanol. The band migrating between CP2 and M4 in *gpi8-1* is a GPI-PLD-, mild base-, and JBAM-sensitive GPI intermediate containing the Man$_4$-GlcN-Ins core,[2] but the structural differences between this species and CP2 or M4 have not been identified.

done as described (39). The generated fragments were analyzed by paper chromatography in methylethyl ketone/pyridine/H_2O (20:12:11) as described (39). Before paper chromatography the products were *N*-acetylated and desalted over mixed-bed ion exchange resin AG-501-X8 (Bio-Rad) unless indicated otherwise (34). Acetolysis was done as described (40). Radiolabeled Man$_x$-GlcNAc-[^{3}H]Ins (x = 1, 2, 3, 4) chromatography standards (Figs. 5 and 6, standards *1–4*) were generated through fragmentation of [^{3}H]Man-labeled head groups of CP2, isolated from *pmi40* by acetolysis then HF, HF then ASAM, JBAM then HF, and HF treatments, respectively. The GlcNAc-[^{3}H]Ins standard (Figs. 5 and 6, standard *0*) was generated by HF treatment of the [^{3}H]Ins-labeled head group of M0, obtained from *sec53* cells. All standards were *N*-acetylated. Dionex HPLC analysis of non-dephosphorylated head groups was done exactly as described (23). Anchor peptides were prepared from labeled proteins as described (23).

Limiting HF Treatment of Head Groups—For limiting HF treatment, aliquots of radiolabeled head groups derived from CP2 and M4 and prepared as above were dephosphorylated with 50 μl of 48% aqueous HF at 0 °C as described (38) for 0–28 h. After neutralization with saturated LiOH, samples were desalted by gel filtration through an 8-ml Sephadex G-10 (Amersham Pharmacia Biotech) column. Samples were then dried in the Speed-Vac and treated with JBAM prior to complete HF dephosphorylation (60 h, 0 °C). Samples were neutralized again with LiOH and *N*-acetylated. Aliquots were dried and then directly applied to Whatman paper No. 1M and analyzed by descending chromatography as described above.

RESULTS

Cloning of GPI7—As reported before (19) and shown in Fig. 2, wild type (wt) cells do not contain polar GPIs (*lane 1*), *gpi8-1* accumulates CP2 as the most polar GPI lipid (*lane 8*), and *gpi7-1* and the *gpi7-1*/*gpi8-1* double mutant accumulate M4 (*lanes 4* and *6*), thus demonstrating that *gpi7-1* is epistatic to *gpi8-1* and suggesting that, during GPI biosynthesis, Gpi7p may act before Gpi8p. Although the original *gpi7* mutants and the unrelated *gpi8-1* mutant were not significantly temperature-sensitive (ts) for growth, the growth of the *gpi7-1*/*gpi8-1* double mutant was strongly temperature-dependent. Transfection of a genomic library into this double mutant allowed the isolation of clones containing complementing plasmids (19).

[2] I. Flury, unpublished observations.

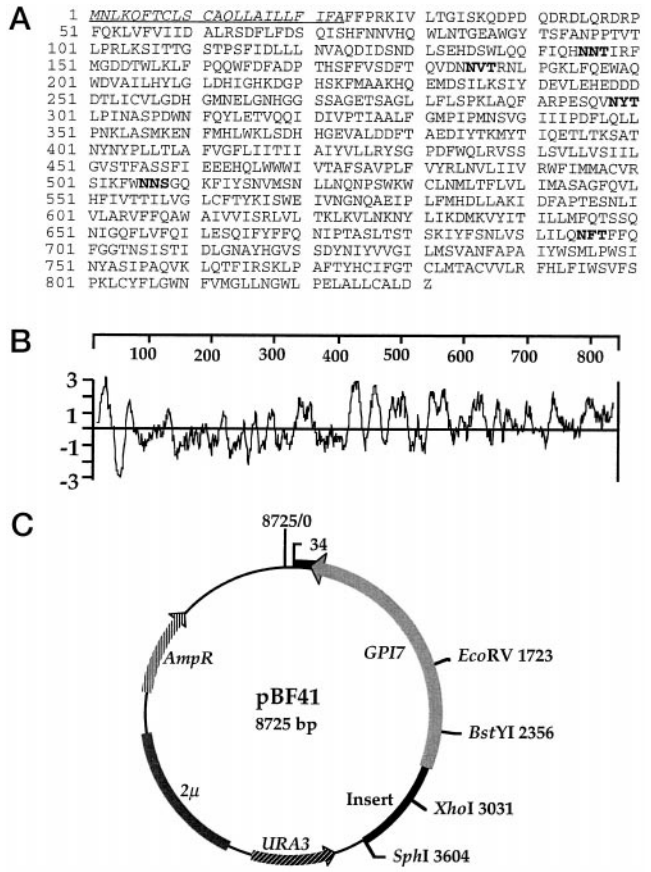

FIG. 3. **Sequence of *GPI7*.** *A,* potential *N*-glycosylation sites are shown in *boldface*. The predicted signal peptide is *underlined*. *B* shows a hydrophobicity plot according to Kyte and Doolittle, in which the hydrophobic sequences get a positive score. *C* shows the restriction map of pBF41. The 3.6-kb *insert* (34–3604) contains *GPI7* (= YJL062w, *broad arrow*). The *Eco*RV/*Bst*YI fragment was expressed in bacteria to get antigen for raising antibodies.

These clones were labeled with *myo*-[^{3}H]inositol ([^{3}H]Ins) at 37 °C, and the lipids were extracted and analyzed by TLC. Upon transfection some *gpi7-1*/*gpi8-1* indeed had regained the ability to make CP2 (Fig. 2, *lanes 6* and *7*) and showed the same lipid profile as *gpi8-1* (Fig. 2, *lane 8*). All these clones harbored plasmids containing YJL062w as the only complete ORF. Transfection of a multicopy vector containing YJL062w under its own promoter (pBF41, Fig. 3*C*) into *gpi7-1* almost completely cured the accumulation of M4 (Fig. 2, *lane 5*). As expected, the accumulation of CP2 by *gpi8-1* was not abolished by the overexpression of YJL062w (Fig. 2, *lanes 8* and *9*). YJL062w predicts an 830-amino acid membrane protein with an N-terminal signal sequence for insertion into the ER, 5 potential *N*-glycosylation sites, and about 9–11 putative transmembrane domains (Fig. 3, *A* and *B*). YJL062w was deleted and replaced by the selectable marker KanMX4. On rich medium the deletants grew about as rapidly as wt cells at all temperatures. Thus, YJL062w is not an essential gene. We were unable to sporulate ΔYJL062/ΔYJL062 diploids indicating that YJL062 is required for sporulation. However, ΔYJL062/YJL062 heterozygotes sporulated readily and ΔYJL062 spores germinated normally. In accordance with previous results on *gpi7* mutants (21), growth of ΔYJL062 (= Δ*gpi7*, see below) on plates at 37 °C was severely inhibited by 0.5 mg/ml Calcofluor White. ΔYJL062 accumulated M4 at even higher levels than *gpi7-1,* and this accumulation was almost completely suppressed by the transfection of pBF41 (Fig. 2, *lanes 2* and *3*). Residual accumulation of M4 may be due to

some cells that lost the complementing plasmid. Transfection of YJL062w under its own promoter on a single copy vector (plasmid pBF43) was sufficient to suppress the accumulation of M4 in a homozygous ΔYJL062/ΔYJL062 diploid (Fig. 2, *lanes 11* and *12*). As can be seen in Fig. 2, *gpi7-1*, ΔYJL062, ΔYJL062/ΔYJL062, and *gpi8-1* mutants also show minor amounts of the GlcNα1,6(acyl→)Ins-P-DAG GPI intermediate M0, the accumulation of which is believed to reflect a build up of GPI intermediates throughout the biosynthetic pathway (Fig. 2, *lanes 2, 4, 6, 8*, and *11*). (It should be noted that some intermediates of intermediate size are obscured on TLC by PI and inositol phosphoceramide (41).) As expected, expression of YJL062w abolishes the accumulation of M0 in *gpi7-1* and ΔYJL062 (Fig. 2, *lanes 3, 5,* and *12*) but not in *gpi7-1*/*gpi8-1* nor *gpi8-1* (*lanes 7* and *9*), since in the latter the GPI biosynthesis remains blocked. To evaluate if the mutation in *gpi7-1* is genetically linked to YJL062w, YJL062w was disrupted in a heterozygous *gpi7-1*/*GPI7* diploid. Correct replacement of one YJL062w locus was verified by PCR in two independent geneticin-resistant transformants. The verified deletants were sporulated, and a total of 26 complete tetrads was labeled with [^{3}H]Ins to analyze the accumulation of M4. In all 26 tetrads only two of the four segregants showed accumulation of M4, whereas the other two showed the lipid profile of wt cells. Geneticin resistance also segregated 2:2 and cosegregated with M4 accumulation in all cases. This demonstrates that the mutation of *gpi7-1* is tightly linked to YJL062w which we henceforth call *GPI7*. Since a construct containing only 348 nucleotides 5′ of the initiation codon of *GPI7* still retained significant complementing activity, we also can dismiss the possibility that the complementing activity of pBF41 is due to one of the two small ORFs located on the opposite strand in the 5′ upstream region of *GPI7* and starting at −409 and −503 with regard to the start codon of *GPI7*.

Characterization of the GPI Intermediate M4—We found that M4, contrary to our initial expectation, contained an HF-sensitive group on Man3 (Fig. 1). Indeed, treatment of the lipid extracts of *gpi7-1* with jack bean α-mannosidase (JBAM, an exomannosidase) shifted M4 to a slightly less hydrophilic position on TLC (Fig. 4*A, lanes 1* and *2*) but not to the position of M0. It seemed conceivable that JBAM did not remove more than one Man from M4 because it was sterically hindered by the detergent micelle in which M4 was embedded. To circumvent this problem, M4 was purified by preparative TLC, and its hydrophilic head group was liberated by GPI-PLD, *O*-deacylated by NH_3, and then subjected to several treatments as indicated at the *top* of Fig. 5, *A–D*. The *N*-acetylated fragment comigrated with the Man_4-GlcNAc-Ins standard (Fig. 5*A*). When treated with JBAM before HF, the resulting *N*-acetylated fragment comigrated with the Man_3-GlcNAc-Ins standard, clearly indicating the presence of a blocking group on Man3 (Fig. 5*B*). The blocking group on Man3 was HF-sensitive, since JBAM done after HF produced a fragment comigrating with GlcNAc-Ins (Fig. 5*C*). *Aspergillus satoi* α-mannosidase (ASAM), a linkage-specific α1,2-exomannosidase, when used after HF treatment, produced Man_2-GlcNAc-Ins (Fig. 5*D*). The migration of the fragments shown in Fig. 5, *A* and *B,* was much slower when *N*-acetylation was omitted (not shown). This partial characterization of M4 is consistent with the presence of a classical Manα1,2(EtN-P→)Manα1,2Manα1,6Manα1,4-GlcNα1,6Ins core structure.

Having recently discovered an additional EtN-P on Man1 of CP2 (22), we considered the possibility that M4 may be lacking EtN-P on Man1. We thus proceeded to compare the non-dephosphorylated head groups of M4 and CP2 by Dionex HPLC using a system in which the presence of negatively charged

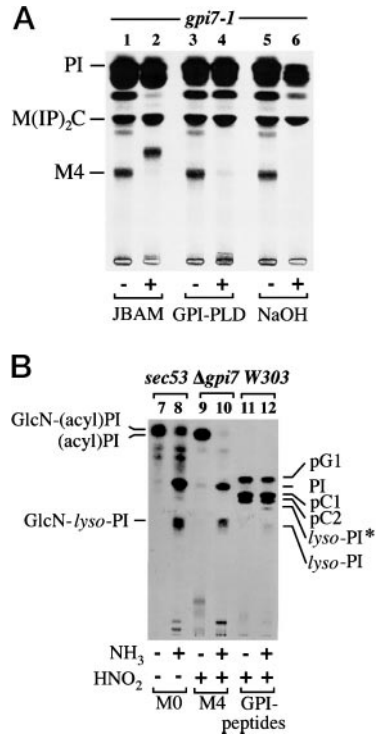

FIG. 4. **Characterization of M4.** *A, gpi7-1* cells were preincubated at 37 °C for 20 min and were labeled with [^{3}H]Ins (2 $\mu Ci/A_{600}$). Lipid extracts were treated (+) or control incubated (−) with either JBAM or GPI-PLD or were deacylated by mild base treatment (NaOH). Desalted products were analyzed by TLC (solvent 2) and fluorography. *B, sec53* and Δ*gpi7* were preincubated and labeled with [^{3}H]Ins at 37 °C (5 $\mu Ci/A_{600}$), and lipid extracts were treated with PI-specific phospholipase C to get rid of labeled PI, and the GPI intermediates M0 and M4 were purified from *sec53* and Δ*gpi7,* respectively, by two rounds of preparative TLC. Anchor peptides were prepared from [^{3}H]Ins-labeled W303 in the experiment described in Table I. M4 and anchor peptides were treated with HNO_2 to liberate the *acyl*-[^{3}H]Ins-P-lipid and [^{3}H]Ins-P-lipid moieties, respectively (Fig. 1). Samples were incubated with (+) or without (−) methanolic NH_3 to remove the acyl from the Ins, desalted and separated by TLC (solvent 1), and processed for fluorography. pG1, protein-derived glycerophospholipid 1; pC1 and pC2, protein-derived ceramides 1 and 2, see Sipos *et al.* (41). Other results of this same experiment were described before (Ref. 41, therein Fig. 2).

phosphodiesters greatly retards the elution of oligosaccharides (42). The non-dephosphorylated head groups of M4 and CP2 eluted as sharp peaks at fractions 22 and 31, respectively (not shown). This wide separation suggested that the head group of M4 contains less negative charge than the one of CP2. To assay directly for a side chain on Man1 of M4, the head group of [^{3}H]Ins-labeled M4 was first cleaved by acetolysis, a procedure which, under mild conditions, selectively cleaves α1,6-glycosidic bonds (Fig. 1). Here this procedure is expected to produce the labeled fragment (*X*-P→?)Manα1,4-GlcNα1,6-[^{3}H]Ins with *X*-P- being the substituent in question. The fragment was then either treated with JBAM or control incubated and finally dephosphorylated by HF, *N*-acetylated, and analyzed by paper chromatography. As can be seen in Fig. 6, *A* and *B*, the (*X*-P→?)Manα1,4GlcNα1,6Ins fragment of M4 is JBAM-resistant, since successive treatment by acetolysis, JBAM, and then HF generates Manα1,4GlcNα1,6Ins. The same had previously been found for CP2 (22). Thus, the difference between the head groups of M4 and CP2 cannot be explained by the presence or absence of an HF-sensitive substituent on Man1: both lipids have the same classical Man_4-GlcN-Ins carbohydrate core structure, they both contain HF sensitive groups on Man1 and Man3 (Fig. 1), but they migrate differently on TLC, and their non-dephosphorylated head groups elute differently on Dionex

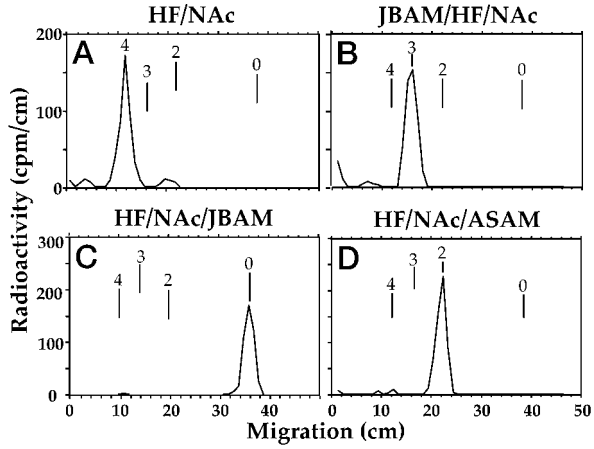

FIG. 5. **Analysis of the head group of M4 using HF, JBAM, and ASAM.** Δ*gpi7* was labeled with [^{3}H]Ins at 37 °C; M4 was purified and used to prepare head groups. Head groups were subjected to HF and *N*-acetylation (*A*); JBAM, then HF, then *N*-acetylation (*B*); HF, then *N*-acetylation, then desalting, then JBAM (*C*); HF, then *N*-acetylation, then desalting, then ASAM (*D*). The thus generated fragments were separated by paper chromatography, and radioactivity contained in 1-cm wide strips was determined through scintillation counting. The position of standards run in parallel on the same paper are indicated: *2–4,* Man_x-GlcNAc-Ins with $x = 2$, 3, or 4. *0,* GlcNAc-Ins.

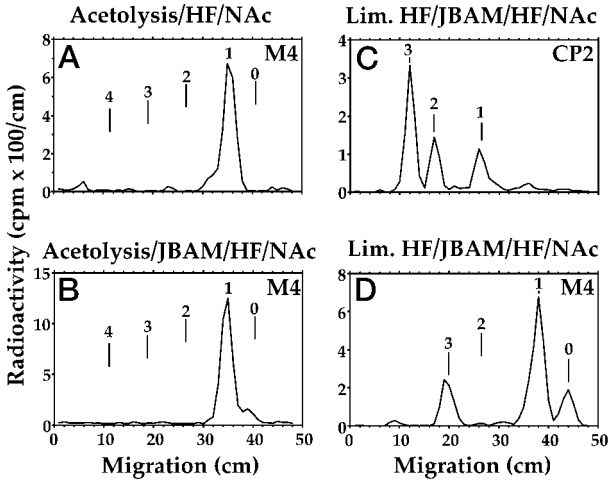

FIG. 6. **M4 of Δ*gpi7* contains an HF-sensitive substituent on Man1 but lacks an HF-sensitive substituent on Man2.** CP2 and M4 head groups were obtained from [^{3}H]Man labeled *pmi40* and [^{3}H]Ins labeled Δ*gpi7,* respectively. *A* and *B*, head groups of M4 were subjected to acetolysis and then either treated with JBAM (*B*) or left untreated (*A*). Finally all products were dephosphorylated with HF, *N*-acetylated, and analyzed by paper chromatography. *C* and *D*, head groups were treated for 12 h with HF, desalted, treated with JBAM, treated with HF for 60 h, *N*-acetylated, and finally analyzed by paper chromatography. Standards *0–4* are Man_x-GlcNAc-Ins ($x = 0, 1, 2, 3, 4$). Free [^{3}H]Man ran out of the paper shown in *C*.

HPLC (data presented above and in Refs. 22 and 23). We thus hypothesized that CP2 may contain either additional HF-sensitive groups on GlcN, Man1, Man2, or Man3 or may contain additional groups linked through the amino group of the EtN-P on M1. Of these several theoretical possibilities, the only ones that have been documented in other organisms are the Man1-P group on the GlcN in *Paramecium aurelia* (43) and the EtN-P group on Man2 in several mammalian GPI proteins, *e.g.* human erythrocyte acetylcholinesterase (44), CD52-II (45), and bovine liver 5′-nucleotidase (46). We used limiting HF treatment to test specifically if CP2 contains an HF-sensitive group on Man2. If we assume that during HF treatment the EtN-Ps are hydrolyzed in a random order, we may expect to find some reaction intermediates lacking the HF-sensitive group on Man3 while retaining EtN-P on Man2 or Man1. When such intermediates subsequently are treated with JBAM and then are dephosphorylated to completeness with HF, they should yield Man_2-GlcN-Ins and Man_1-GlcN-Ins fragments, respectively. For preliminary tests, CP2 head groups were first treated with HF for 0.5, 1, 3, 9, 12, 18, or 28 h, then with JBAM, and finally with HF for 60 h. These experiments showed that both Man_2-GlcN-Ins and Man_1-GlcN-Ins fragments became visible after 1 h of limiting HF treatment, peaked at 12 h, and remained detectable at all time points up to 28 h. In quantitative terms it appeared that Man_3-GlcN-Ins $>$ Man_2-GlcN-Ins $\geq$ Man_1-GlcN-Ins at all time points. Importantly, treatment of the head group of CP2 with HF for 12 h yielded substantial amounts of Man_2-GlcN-Ins and Man_1-GlcN-Ins (Fig. 6*C*), whereas the identical treatment performed with the head group of M4 only yielded Man_1-GlcN-Ins but no Man_2-GlcN-Ins (Fig. 6*D*). This result is compatible with the idea that Δ*gpi7* cells are unable to add an HF-sensitive group onto Man2 of the GPI core (Fig. 1). It also confirms the presence of an HF-sensitive group on Man1 of both M4 and CP2.

The Lipid Moieties of GPI Intermediates in Δgpi7 Are Normal—We looked for additional differences between M4 and CP2 by analyzing the lipid moiety of M4. M4 is sensitive to GPI-specific phospholipase D (GPI-PLD) and mild base treatment (Fig. 4*A, lanes 3–6*), suggesting that its lipid moiety consists of Ins-P-DAG. We previously reported that M4 is resistant to PI-specific phospholipase C (21). This finding, together with the GPI-PLD sensitivity, can be taken as an indication for the presence of an acyl moiety attached to the Ins of M4. We further released the (acyl→)Ins-P-DAG moiety of M4 with HNO_2 as described recently (41). As shown in Fig. 4*B*, the treatment of purified M4 by HNO_2 produced a very hydrophobic species, which migrates very closely to M0, *i.e.* the GlcN(acyl→)Ins-P-DAG accumulating in *sec53* (Fig. 4*B, lanes 7* and *9*) (41). (As reported previously, the presence of GlcN on these early precursors does not significantly influence their migration in TLC, for discussion see Sipos *et al.* (41).) Partial deacylation of the M4-derived lipid moiety by NH_3 produced PI and lyso-PI (Fig. 4*B, lane 10*). This PI was compared with pG1, the PI species obtained by HNO_2 treatment of protein-bound GPI anchors from the corresponding wt strain (Fig. 4*B, lane 11*). The comparison shows that M4 contains a PI moiety that migrates clearly less than pG1, whereas a lyso-PI of M4 migrates slightly more than the lyso-PI species generated by methanolic NH_3 treatment of anchor peptides (Fig. 4*B, lanes 10* and *12*). Very similar results had been obtained previously when comparing protein-derived PI moieties with the PI moieties of M0 from *sec53* and of CP2 from *gpi8-1* (41). In addition we isolated from Δ*gpi7* the recently identified GPI intermediates that are obscured in TLC by PI and inositol phosphoceramides (Ref. 41, therein Fig. 6*A*), and we found that they are exactly the same as the corresponding intermediates from wt cells by all criteria (not shown). Thus, it seems that M4 and other GPI intermediates of Δ*gpi7* contain the same PI moiety as early and late GPI intermediates accumulating in other mutants or in wt cells, and we therefore conclude that the difference between CP2 and M4 is solely due the difference in their head groups.

Lack of Gpi7p Affects the in Vitro Biosynthesis of GPI Precursor Lipids—When yeast microsomes are incubated in the presence of UDP-[^{3}H]GlcNAc, ATP, coenzyme A, GDP-Man, and tunicamycin, they generate labeled GPI intermediates as the only kind of labeled lipids (22, 47). Wild type microsomes make GPI intermediates up to CP2. Although a large array of incomplete intermediates is also generated, the pattern of labeled intermediates is fairly reproducible. When we used Δ*gpi7*

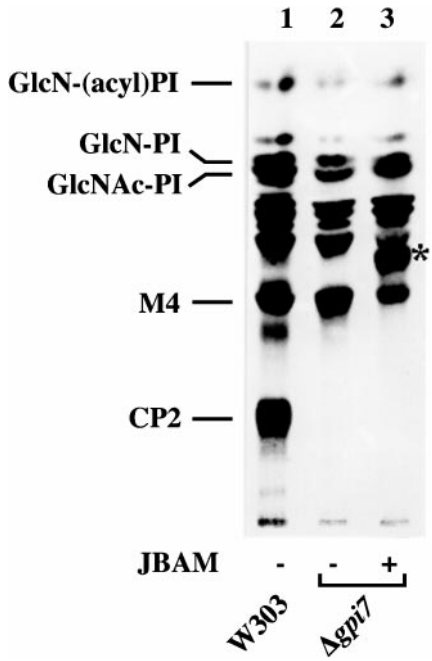

FIG. 7. **Microsomes of Δ*gpi7* synthesize M4 and not CP2.** Microsomes of W303 wild type or Δ*gpi7* were incubated with 6 μCi of UDP-[^{3}H]GlcNAc, GDP-Man, tunicamycin, and ATP for 1 h at 37 °C as described (22). The glycolipid products were extracted and then run on TLC with solvent 2. The extract in *lane 3* was first treated with JBAM. On the basis of the preceding analysis the band denoted with an *asterisk* can be presumed to be an M4 derivative in which Man4 has been removed.

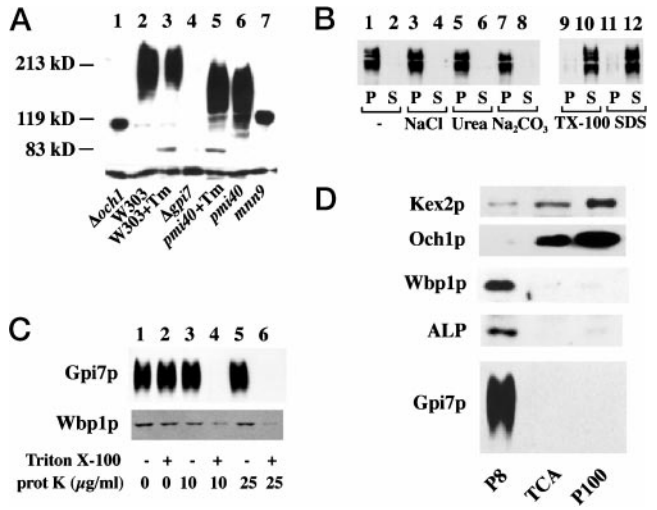

FIG. 8. **Membrane association, orientation, and localization of Gpi7p.** *A,* exponentially growing cells were broken with glass beads in TEPI buffer as described (19); lysates were centrifuged at 10,000 × *g* for 15 min at 4 °C, and microsomal pellets were processed for SDS-PAGE. Cells in *lanes 3* and *5* had been grown in 20 μg/ml tunicamycin (*Tm*) for 90 min. *B–D*, exponentially growing W303 cells were broken with glass beads using the buffers indicated under "Experimental Procedures," and cell wall debris was removed by centrifugation at 600 × *g*. *B*, aliquots of cell lysate were incubated for 30 min at 0 °C with 0.5 M NaCl, 0.8 M urea, 1% Triton X-100 (*TX-100*), 0.1 M Na_2CO_3, pH 11, or 1% SDS. Subsequently membranes were sedimented by ultracentrifugation to get supernatant (*S*) and pellet (*P*) fractions. *C*, cell lysate was sedimented at 13,000 × *g* for 15 min, and the membrane pellet was thoroughly resuspended and digested with 10 or 25 μg/ml proteinase K (*prot K*) at 0 °C for 20 min in the presence or absence of 0.5% Triton X-100. *D*, cell lysates were subjected to differential centrifugations at 8,000 and 100,000 × *g*. These centrifugations generated pellet P8 containing ER, PM, and vacuolar membranes and pellet P100 which contains Golgi membranes. The 8,000 × *g* supernatant was also precipitated with trichloroacetic acid (*TCA*). In all panels the lanes contain material derived from 1 A_{600} of cells except for *lanes 1* and *7* of *A* which contain 0.3 A_{600}.

microsomes, they reproducibly made all the normal intermediates down to a band comigrating with M4 of [^{3}H]Ins-labeled Δ*gpi7* cells, but they consistently failed to make CP2 (Fig. 7). When the labeled lipid extract was treated with JBAM, most of the band comigrating with M4 was shifted to a less hydrophilic position, much in the same way as seen for [^{3}H]Ins-labeled M4 (Fig. 2, *lanes 1* and *2*). Thus, the M4 accumulation of Δ*gpi7* can be reproduced *in vitro*. This result implies that the Gpi7p present in wt microsomes is functional *in vitro*.

Characterization of Gpi7p—Gpi7p was characterized using affinity purified rabbit antibody made against the N-terminal, hydrophilic part of *GPI7* (Fig. 3*B*). As shown in Fig. 8*A*, the antibody recognized a heterogeneously glycosylated 208-kDa protein, the estimated molecular mass of various glycoforms ranging, after heavy exposure, from about 130 to 230 kDa (Fig. 8*A, lane 2*). The predicted mass of the protein before and after removal of the signal sequence is 94,832 and 92,207 Da, respectively. In glycosylation mutants Δ*och1*/*mnn1* or *mnn9* which are totally or partially deficient in the elongation of *N*-glycans in the Golgi, Gpi7p has an estimated mass of 108 and 115 kDa, respectively (Fig. 8*A, lanes 1* and *7*). *pmi40* has a ts deficiency in Man biosynthesis that is partial at 24 °C (48). In *pmi40* grown at 24 °C the average mass of Gpi7p is around 150 kDa (Fig. 8*A, lane 6*). (This suggests that full elongation of *N*-glycans is not necessary for Gpi7p function since, when shifted from 24 to 37 °C, *pmi40* cells are able to make CP2 (23).) Tunicamycin treatment of wt or *pmi40* cells resulted in the appearance of a single, relatively sharp band of an apparent molecular mass of about 83 kDa (Fig. 8*A, lanes 3* and *5*). The protein could also be deglycosylated to an apparent molecular mass of 86 kDa by treatment with endoglycosidase H (not shown). All these data concurrently indicate that Gpi7p contains several *N*-glycans that are heavily elongated in the Golgi but contains no or only few *O*-glycans. In the cell lysate Gpi7p was rapidly degraded by an endogenous protease which, however, could be inhibited by 10 mM EDTA. Gpi7p is associated with membranes since it could be sedimented by ultracentrifugation of lysates at 100,000 × *g* for 60 min (Fig. 8*B, lanes 1* and *2*). Gpi7p was neither dissociated from membranes by NaCl nor sodium carbonate at pH 11, nor urea, but it was efficiently solubilized by Triton X-100 or SDS (Fig. 8*B*). The presence of an N-terminal signal sequence and the large amount of *N*-glycans suggested that the hydrophilic N-terminal part of the protein, which contains 3 of the 5 potential *N*-glycosylation sites, would reside on the lumenal or ectocytoplasmic side of the membrane. We tried to confirm this orientation by protease protection assays on microsomes. As shown in Fig. 8*C*, neither Gpi7p nor Wbp1p, which was used as a control, were degraded by proteinase K unless microsomes were permeabilized with Triton X-100. Wbp1p has been demonstrated to be a lumenal ER protein (49), and our result thus shows that the N-terminal hydrophilic part of Gpi7p is not accessible to protease in these microsomes. It is noteworthy that proteinase K did not reduce the molecular mass of Gpi7p, thus indicating that the cytosolic loops between the predicted transmembrane domains of the C-terminal part of Gpi7p are not accessible to proteinase K in native microsomes.

The cellular localization of Gpi7p was investigated by subcellular fractionation as shown in Fig. 8*D*. Differential centrifugation at 8,000 and 100,000 × *g* for 10 and 60 min, respectively, achieved satisfactory separation of the Golgi markers Kex2p and Och1p from the ER marker Wbp1p and from the vacuolar alkaline phosphatase. We were concerned that the relative amounts of these proteins in the 100,000 × *g* pellet

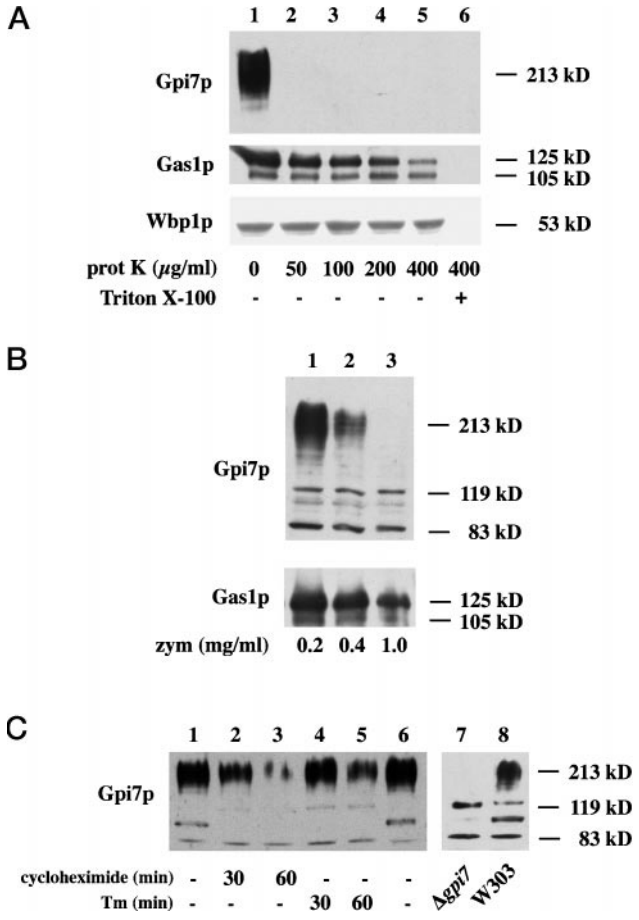

FIG. 9. **Gpi7p is localized at the cell surface.** Cells in the early exponential phase growing at 30 °C in YPD were used. *A*, intact W303 cells were treated with cysteamine chloride and then treated with the indicated concentrations of proteinase K (*prot K*) exactly as described (65) except that the EDTA concentration was raised to 20 mM. In *lane 6*, Triton X-100 was added to 1%. *B*, W303 cells were treated with zymolyase 20T at the indicated concentrations. *C*, W303 or Δ*gpi7* cells were either lysed directly or after having been incubated for 30 or 60 min at 10 A_{600}/ml in the presence of cycloheximide (200 μg/ml) or tunicamycin (*Tm*, 20 μg/ml). Cells were lysed by boiling in sample buffer and processed for SDS-PAGE and Western blotting with antibodies against Gpi7p, Gas1p, or Wbp1p.

may be underestimated due to ongoing proteolytic degradation during the 100,000 × *g* spin. Therefore the supernatant of the 8,000 × *g* spin was split whereby proteins were immediately precipitated with trichloroacetic acid in one half, and the other half was pelleted at 100,000 × *g*. Gpi7p was exclusively found in the 8,000 × *g* pellet (P8) and thus is associated with either the ER, the vacuole, or the PM but not with the Golgi. As shown in Fig. 9*A* low amounts of proteinase K added to intact cells hydrolyzed all of the mature Gpi7p. In contrast, Wbp1p and the 105-kDa ER form of Gas1p were completely resistant to this treatment unless membranes were permeabilized with Triton X-100 (Fig. 9*A, lane 6*). The mature 125-kDa form of Gas1p was found to be partially resistant to proteinase K, indicating either a tighter interaction of Gas1p with some cell wall components or the existence of an internal pool of Gas1p as proposed earlier (50). Crude zymolyase treatment of intact cells also removed all of the mature form of Gpi7p (Fig. 9*B*), whereas recombinant zymolyase left Gpi7p intact (not shown). Longer exposures showed the presence of several minor bands of smaller size all of which were also present in Δ*gpi7* cells except for a 108-kDa form of Gpi7p (Fig. 9*C, lanes 7* and *8*). This material seems to be an ER form in transit to the surface since it was no more detectable if cells were preincubated with either cycloheximide

TABLE I
Quantitation of GPI anchor lipids

Cells were labeled with [^{3}H]Ins (5 μCi/A_{600}) for 75 min at 37 °C. Incorporation of [^{3}H]Ins into lipids ranged from 43 to 49% of the radioactivity added to cells. Proteins were extensively delipidated, and anchor peptides were prepared as described (41). Anchor peptides were treated with HNO_2 to liberate the [^{3}H]Ins-P-lipid moieties; the products were desalted by partitioning between butanol and water, and the labeled lipid products were separated by TLC and quantitated by radioscanning. Results of the quantitation of anchor lipids pG1, pC1, and pC2 are given as percentage of the total radioactivity of anchor peptides. The remaining 7–11% that are not accounted for stayed at the origin and represent residual anchor peptides that had not been cleaved by HNO_2 treatment. An aliquot of W303 anchor lipids is shown in Fig. 4*B, lane 11*.

	pG1	pC1	pC2
W303	22.2	63.6	7.4
X2180	24.2	61.2	4.8
gpi8–1	23.8	63.9	2.6
Δ*gpi7*	68.8	19.3	1.1

or tunicamycin (Fig. 9*C, lanes 1–6*). These data also indicate that mature Gpi7p is relatively rapidly degraded or becomes resistant to extraction with SDS. Globally these data indicate that the bulk of Gpi7p is exposed at the cell surface but that a small amount of core-glycosylated material is found in the ER in transit to the cell surface. For the moment it is unclear why Gpi7p was completely protected in microsomes, since it has been claimed that PM does not form closed vesicles upon homogenization (51). It is conceivable that Gpi7p resides in special PM subdomains that form closed vesicles upon homogenization or that centrifugation of microsomes generated protease-resistant membrane aggregates (51).

Deletion of GPI7 Alters GPI Protein Transport and Remodeling—We previously reported on the accumulation of the immature 105-kDa ER form of Gas1p in *gpi7* mutants (21). We therefore investigated GPI protein transport in Δ*gpi7*. Indeed, by pulse-chase experiments we found that the maturation of GPI proteins Sag1p and Gas1p was slowed 2–3-fold as compared with wt cells, whereas the maturation of carboxypeptidase Y proceeded with normal kinetics (not shown). This indicates that the transport of GPI proteins in Δ*gpi7* is specifically retarded. Nevertheless, in rich media Δ*gpi7* cells grow at roughly the same rate as wt cells. They also incorporate [^{3}H]Ins with the same efficiency as wt cells.

The lipid remodeling of GPI anchors is significantly altered in Δ*gpi7*. As seen in Table I, the proportion of ceramides (pC1 and pC2) in anchor peptides from Δ*gpi7* is drastically decreased, whereas the fraction of DAG-containing lipids ((pG1) is correspondingly increased. It should be noted that at the time of analysis, *i.e.* 75 min after addition of [^{3}H]Ins, the relative amounts of mild base-sensitive and mild base-resistant anchors are no longer changing and represent the steady state proportion of these two anchor types (41, 52). It is important to realize that pG1 also represents a remodeled form of the anchor lipid in which a long chain fatty acid has replaced the original fatty acid present in *sn*-2 of the glycerol of the CP (Fig. 1). It thus appears that the relative decrease of ceramide remodeling goes along with a compensatory increase in DAG remodeling. A relative reduction in ceramide remodeling was also observed when we compared the efficiency of [^{3}H]Ins and [^{3}H]dihydrosphingosine ([^{3}H]DHS) incorporation into GPI proteins. As can be seen in Fig. 10, the ratio of [^{3}H]DHS/[^{3}H]Ins incorporation into proteins is much higher in wt than in Δ*gpi7* (Fig. 10, *lanes 1–4*). The lack of incorporation of [^{3}H]DHS in Δ*gpi7* cannot be explained by an increase of the endogenous production of DHS in Δ*gpi7*, since the difference between wt and Δ*gpi7* persists, even when all endogenous DHS biosynthesis is blocked by myriocin (Fig. 10, *lanes 5* and *6*). The defect in

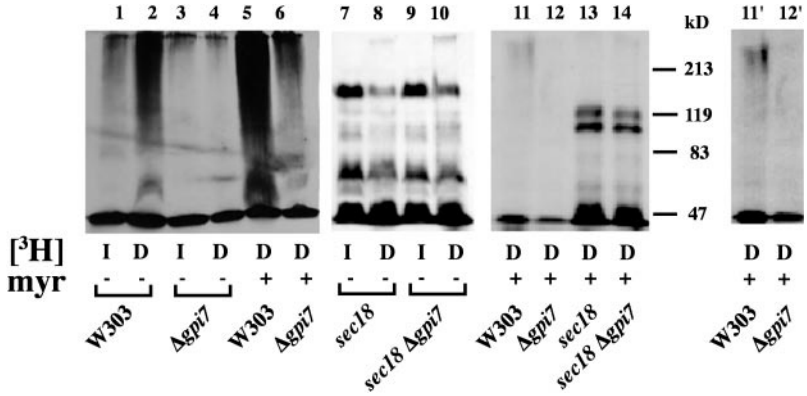

FIG. 10. **Ceramide remodeling of GPI anchors is reduced in Δ*gpi7*.** Cells growing exponentially in SDCUA were used. Cells were labeled by the addition of either 25 μCi of [^{3}H]DHS (*D*) or [^{3}H]Ins (*I*) to an aliquot of 2.5 A_{600} of cells exactly as described (24). *Lanes 1–6*, precultures and labelings were at 30 °C. Cells were preincubated with (+) or without (−) 40 μg/ml of myriocin (*myr*) for 20 min before addition of the radiotracers. *Lanes 7–10*, *sec18* or *sec18* Δ*gpi7* double mutants were precultured at 24 °C and preincubated for 10 min at 37 °C before addition of the tracers. *Lanes 11–14*, cells were labeled in the presence of cycloheximide under conditions in which only the Golgi/PM remodelase (*lanes 11* and *12*) or only the ER remodelase (*lanes 13* and *14*) is probed (Ref. 24, therein Fig. 7 (Golgi/PM remodelase) and Fig. 8 (ER remodelase)). All samples were processed for SDS-PAGE under reducing conditions and fluorography. *Lanes 11′* and *12′* were scanned at an increased sensitivity.

remodeling seems to be affecting mostly the maturation processes in the Golgi and/or PM (Golgi/PM remodeling) since, as shown in Fig. 10, *lanes 7–10*, the ratio of [^{3}H]DHS/[^{3}H]Ins incorporation into proteins in the Δ*gpi7*/*sec18* double mutant was the same as in *sec18*. Also, when using stringent conditions under which one observes only ER or only Golgi/PM remodelase (24), remodeling in the ER appeared relatively normal, whereas remodeling in the Golgi/PM was reduced (Fig. 10, *lanes 11–14, 11′,* and *12′*). The relatively low amount of pC2 in anchor lipids of Δ*gpi7* (Table I) may be a consequence of this relative deficiency of Golgi/PM remodeling, since pC2 type anchors are only generated by the Golgi/PM but not the ER remodelase (24, 41). The relationship between the specific retardation of GPI protein transport, reduced Golgi/PM remodeling, and increased remodeling toward pG1 is for the moment unclear.

DISCUSSION

Yeast and mammals contain the same GPI carbohydrate core structure. This suggests that the GPI anchoring pathway has been established early in evolution and has rigorously been conserved in widely diverging organisms. On the other hand, the side chains added to this core as well as the lipid moieties of the anchor tend to vary a lot between different species (1). The GPI anchors of *S. cerevisiae* contain two types of side chains as follows: one or two mannoses are linked to Man3 (53) and an EtN-P side chain is linked to Man1.[3] Both side chains are already present on the precursor lipid CP2 (22, 23). These two side chains are also found in some vertebrates, including mammals, and possibly in *Dictyostelium discoideum* (1), suggesting that not only the GPI core structure but also certain kinds of side chains have been invented in and conserved since early times of evolution. Here we present evidence for yet a further, possibly conserved HF-sensitive substituent on CP2 which is attached to Man2. So far, the only side chain attached to Man2 reported in the literature is EtN-P. EtN-P was found by mass spectrometry on 15% of anchors of human erythrocyte cholinesterase and 3% of bovine liver 5′-nucleotidase (44, 46). Partial acid hydrolysis has also indicated an HF-sensitive substituent on Man2 in 40% of CD52-II (45). Analysis of the ethanolamine/Ins ratio in GPI anchors of porcine renal membrane dipeptidase and of human placental alkaline phosphatase yielded values of 2.5 and 2.4, suggesting the presence of EtN-P on Man2 in 50 and 40% of their anchors, respectively (54, 55). However, no such side chain was detected in other mammalian GPI proteins such as rat brain Thy-1 glycoprotein (56) or hamster scrapie prion (57). It may be that in many studies part or all of EtN-P side chains on Man2 and Man1 were hydrolyzed by an unspecific phosphodiesterase during the purification of the respective GPI proteins and preparation of anchor peptides using Pronase. Such a phosphodiesterase activity may explain why we failed to detect any EtN-P side chain on GPI-anchored yeast proteins in the past (53), although we now have firm evidence for the presence of an HF-sensitive substituent on Man1.[3] The chemical nature of the side chain on Man2 of CP2 remains to be determined. The presence of an HF-sensitive side chain on Man2 of CP2 has its parallel in human cells. Indeed, there is evidence for an HF-sensitive group on Man2 of H8, the most polar GPI lipid of HeLa cells (58). The EtN-P side chains on Man1 and Man3 being conserved between mammalian organisms and yeast, it appears reasonable to speculate at this point that the analogy between mammalian and yeast anchors may extend to the substituent on Man2, *i.e.* that also the side chain on Man2 of yeast GPI structures may consist of an EtN-P and that this EtN-P may be present on some mature GPI proteins of *S. cerevisiae*.

Δ*gpi7* cells are hypersensitive to Calcofluor White and hence have some difficulty in constructing their cell walls. Several reasons can be envisaged. (i) The side chain on Man2 may be important for the interaction of CPs with the transamidase complex and for their efficient transfer onto proteins. Recent data show that a small reduction of Gpi8p renders transamidase activity rate-limiting.[3] The synthetic effect of *gpi7* mutations with *gpi8* mutations suggests that deletion of *GPI7* may have a similar effect. A decreased transamidase activity may particularly affect the anchoring of certain GPI proteins that have a low affinity for the transamidase even though the global rate of GPI biosynthesis and [^{3}H]Ins incorporation into proteins of Δ*gpi7* is not grossly reduced. Thus it is conceivable that some GPI proteins important for cell wall architecture are lacking in Δ*gpi7*. (ii) The side chain on Man2 may serve as an attachment point for the covalent linkage of β1,6-glucans to the anchor moiety of cell wall proteins although a recent analysis of the linkage region between the GPI anchor remnant and β1,6-glucans rather showed a direct glycosidic linkage between Man1 and the β1,6-glucan (6). (iii) The side chain may serve as a recognition signal for enzymes or proteins that facilitate the packaging of GPI proteins into vesicles, for remodelases that

[3] I. Imhof, U. Meyer, A. Benachour, I. Flury, E. Canivenc-Gansel, C. Vionnet, and A. Conzelmann, manuscript in preparation.

TABLE II
GPI7 has homologues in other species

Homologous sequences were compared by ClustalW at the European Bioinformatics Institute (www2.ebi.ac.uk/clustalw/). The aligned scores for pairwise alignments are reported; a high score indicates high homology. ORFs that have not received gene names are indicated by their chromosomal denominator (S. cerevisiae) or the NCBI protein identification number (PID). Subfamilies are separated by blank lines. Alignments within a given subfamily are in bold. *S.c., S. cerevisiae; S.p., Schizosaccharomyces pombe.*

		1	2	3	4	5	6	7	8	9
1	YJL062w = *GPI7, S.c.*									
2	*YA93*, (1175452), *S.p.*	**29**								
3	(1132507), *C. elegans*	**22**	**26**							
4	YLL031c, *S.c.*	22	19	16						
5	(2984587) *homo sapiens*	18	20	16	**24**					
6	(2257562) *S.p.*	20	20	18	**28**	**23**				
7	(2734088) *C. elegans*	19	19	16	**21**	**20**	**23**			
8	*MCD4*, YKL165c *S.c.*	15	15	18	12	12	14	12		
9	(2879870) *S.p.*	16	14	14	12	11	13	1	**39**	

exchange their lipid moieties, or for hydrolases or transglycosidases that remove parts of the GPI anchor of cell wall proteins and hook the GPI remnant onto β1,6-glucans (4, 5).

Our data further show that ceramide remodeling in the Golgi/PM is significantly reduced in Δ*gpi7,* whereas remodeling toward pG1 is increased whereby it is not clear if pG1 remodeling is increased because ceramide remodeling is decreased or if ceramide remodeling is decreased because pG1 remodeling is increased. Moreover, the relationship of the alteration of GPI remodeling with the other phenotypic changes of Δ*gpi7*can be explained in several ways. (i) Previous studies showed that remodeling toward pG1 occurs in the ER and that retention of GPI proteins in the ER in secretion mutants maintains a high pG1/pC1 ratio on these proteins (41). Thus, if the substituent on Man2 of GPI anchors is important for efficient packaging of GPI proteins into transport vesicles, the delay in export of GPI proteins out of the ER may give the ER remodelase generating pG1 prolonged access to the GPI proteins and may thus cause a relative increase of pG1. (ii) The side chain on Man2 may serve as a recognition signal for Golgi/PM remodelase. (iii) We also considered the possibility that Gpi7p itself may be a Golgi/PM remodelase. This latter hypothesis would not directly explain why Δ*gpi7* cells cannot attach the HF-sensitive substituent onto Man2 and would imply that the addition of this side chain somehow is directed by the prior attachment of a ceramide moiety. This, however, is clearly not the case, since CP2 also contains the HF-sensitive side chain on Man2, although its lipid moiety consists of DAG (23). Thus we believe that the reduced Golgi/PM remodeling of GPI proteins in Δ*gpi7* is secondary to the lack of a substituent on Man2.

Our previous data suggested that CP2 can be transferred to proteins (23), and our working hypothesis until recently assumed that CP2 represents the GPI lipid used for GPI anchoring also by normal cells that do not accumulate this lipid ("CP2 hypothesis"). By consequence we would have predicted that all the enzymes required for the elaboration of CP2 are localized in the ER. Paradoxically, the subcellular fractionation experiments and protease treatment of intact spheroplasts strongly suggest that the bulk of Gpi7p resides at the cell surface (Fig. 9, *A* and *B*). Moreover, although we recently succeeded in demonstrating the presence of an HF-sensitive group on Man1 of immature ER forms of GPI proteins, we presently lack the tools to look for such a group on Man2. Thus, the so far available data raise a doubt whether it is CP2 which is added to GPI proteins in the ER, and we therefore are presently considering the possibility that other GPI lipids than CP2 are the physiological substrate of the ER transamidase. In fact, neither CP2 nor M4 can be detected in wt cells. It therefore seems possible that under physiological conditions cells add M4 to GPI proteins ("M4 hypothesis") and that CP2 is elaborated only in mutants in which M4 cannot be transferred to proteins, spills out of the ER, and reaches the PM. It is noteworthy that Δ*gpi7* incorporates [^{3}H]Ins at a normal rate into proteins suggesting that the transamidase is perfectly able to transfer M4. Thus, the side chain on Man2 may normally not be added to GPI proteins or only be added after GPI proteins arrive at the cell surface. The M4 hypothesis, however, does not explain why M0 and M4 accumulate in Δ*gpi7,* whereas M0, M4, and CP2 remain undetectable in wt cells (Fig. 2, *lanes 1* and *2*) or why *gpi8-1*, deficient in the transfer of GPIs onto proteins, accumulates CP2 (19, 21). It also fails to explain the delayed maturation of GPI proteins and the reduced rate of GPI remodeling observed in Δ*gpi7.* To save the M4 hypothesis, the accumulation of GPI intermediates in Δ*gpi7* could be rationalized by assuming that the substituent on Man2 serves to mark supernumerary GPIs for degradation, but also this assumption does not explain the observed accumulation of CP2 in *gpi8*. Thus, although our results raised the possibility that M4 is the physiological GPI lipid for GPI anchoring, this M4 hypothesis leaves many results unexplained and the data are more easily explained by our original CP2 hypothesis. For one, the synchronous accumulation of M4 and CP2 in all our *gpi8* mutants argues that M4 is not a better substrate for the transamidase than CP2. CP2 may physiologically be produced by the small amount of Gpi7p in the ER (Fig. 9*C*). Alternatively, it is conceivable that M4 is transported from the ER to the PM, is converted there to CP2, and is then transported back to the ER by some not yet elucidated mechanism. In this context it is noteworthy that the biosynthesis of GPIs by wt microsomes *in vitro* produces CP2 in good yield, *i.e.* the *in vitro* system adds the substituent on Man2. This *in vitro* system does not contain cytosol nor GTP and hence should not support vesicular transport from ER- to Golgi-derived microsomes (59). It is possible, however, that GPI lipids are transported between microsomes or membrane fragments by means of lipid transfer proteins or through direct contact between membranes. It also can be envisaged that juxtaposition of membranes allows enzymes present in one membrane to work on lipids in another membrane. The same mechanisms may also operate in intact cells. Clearly the identity of the physiological GPI lipid substrate of the transamidase will have to be established by further experiments.

Homology searches show that two ORFs of *S. cerevisiae* are related to *GPI7*, *MCD4* (= YKL165c), and YLL031c. They belong to a novel gene family comprising for the moment the nine members shown in Table II which, based on the many predicted transmembrane domains, were previously classified as putative permeases (60). Pairwise alignment allows us to group

them into three subfamilies of more closely related ORFs. All nine ORFs predict membrane proteins of about 100 kDa having an N-terminal signal sequence, a hydrophilic N-terminal part, and multiple transmembrane domains in their C-terminal half. *mcd4* mutants were obtained in a screen for cells deficient in the cell cycle controlled polarization of growth, a phenotype also generated by mutations in the exocyst or in *N*-glycosylation (61). The subfamilies typified by *GPI7* and YLL031c are more closely related to each other than to the *MCD4* subfamily. All nine family members contain two conserved motifs at about the same position in the hydrophilic N-terminal domain, namely H*X*LGXD*XX*GH and DHGM*XXX*G*X*HG. These motifs are also found in two EST clones from human cDNA that have high homology to *MCD4* (NCBI PID 1779747 and 1765215, ClustalW alignments giving aligned scores of 46 and 35). Very interestingly, by a reiterated Psi Blast search at the National Center of Biotechnology Information (NCBI) (62) one can find a highly significant homology of all three subfamilies with a large family of phosphodiesterases. The large majority of these homologous sequences encode mammalian cell-surface proteins classified as alkaline phosphodiesterase I, nucleotide pyrophosphatase, or alkaline phosphatase. The homology comprises a region of about 220–240 amino acids in the N-terminal hydrophilic part of *GPI7*, YLL031c, and *MDC4*. The homology of *GPI7* in this region with mammalian and plant phosphodiesterases amounts to 17–18% identity and 30–34% similarity and comprises a motif PT*X*TX$_8$TG*X*$_2$P which is common to bacterial, viral, plant, and mammalian phosphodiesterases. This homology may suggest that Gpi7p itself is the transferase adding the phosphodiester-linked substituent on Man2. In this context it is interesting to note that the EtN-P on Man3 of the GPI anchor has been shown to be transferred by transesterification using phosphatidylethanolamine as donor of EtN-P (63, 64). Mutants in YLL031c also accumulate abnormal GPI intermediates which on TLC have about the same mobility as M4 suggesting that YLL031c is similarly involved in adding EtN-P.[2] Thus, it is conceivable that not only the *GPI7* subfamily but also other subfamilies are involved in the transfer of EtN-P onto the GPI core structure. However, the transesterification activity of Gpi7p will have to be shown directly before one can exclude that the primary function of Gpi7p is to generate some signal from the cell wall which regulates GPI protein transport and remodeling as well as side chain addition to GPI structures.

It is interesting that subfamily members belonging to different species are more closely related to each other than family members belonging to a single species. This can be seen when comparing the pairwise alignment scores among the three ORFs of *S. cerevisiae* or the three ORFs of *Schizosaccharomyces pombe* with the scores among subfamily members (Table II). In evolutionary terms this suggests that the divergence of these three subfamilies occurred earlier than the separation of the lineages leading to *S. cerevisiae*, *S. pombe,* and *Caenorhabditis elegans*. This implies that the HF-sensitive group on Man2 is of very ancient origin. *GPI7* bears no resemblance with *PIG-F*, a mammalian gene encoding for a highly hydrophobic membrane protein involved in the addition of EtN-P to Man3 (10). The exact role of PIG-F has not yet been elucidated.

It will be interesting to find the human homologues of *GPI7*. It may be that this gene, as in *S. cerevisiae*, plays a more dispensable role in GPI anchoring than the enzymes involved in the elaboration of the carbohydrate core structure such as for instance *PIG-A*/*GPI3*/*CWH6*/*SPT14* (7). Thus, although deficiencies in *PIG-A* are only acquired by somatic cells, deficiencies in the human *GPI7* homologue may be transmittable through the germ line as well.

Acknowledgments—We are grateful to Dr. N. Rao Movva for myriocin; and Dr. R. Fuller, Dr. Y. Jigami, Dr. S. Emr, Dr. M. Aebi, Dr. M. Payton, Dr. H. Riezman, and Dr. R. Schekman for antibodies and yeast strains. We are grateful to Dr J. van Oostrum (Novartis, Basel, Switzerland) for giving us access to and helping with the Dionex HPLC. We especially thank Dr. S. Munro, MRC, Cambridge, UK, for pointing out the homology between *GPI7* and the phosphodiesterase family.

REFERENCES

1. McConville, M. J., and Ferguson, M. A. (1993) *Biochem. J.* **294,** 305–324
2. Hamada, K., Fukuchi, S., Arisawa, M., Baba, M., and Kitada, K. (1998) *Mol. Gen. Genet.* **258,** 53–59
3. Caro, L. H., Tettelin, H., Vossen, J. H., Ram, A. F., van den Ende, H., and Klis, F. M. (1997) *Yeast* **13,** 1477–1489
4. Lu, C.-F., Montijn, R. C., Brown, J. L., Klis, F., Kurjan, J., Bussey, H., and Lipke, P. N. (1995) *J. Cell Biol.* **128,** 333–340
5. de-Nobel, H., and Lipke, P. N. (1994) *Trends Cell Biol.* **4,** 42–45
6. Kollar, R., Reinhold, B. B., Petrakova, E., Yeh, H. J., Ashwell, G., Drgonova, J., Kapteyn, J. C., Klis, F. M., and Cabib, E. (1997) *J. Biol. Chem.* **272,** 17762–17775
7. Takeda, J., and Kinoshita, T. (1995) *Trends Biochem. Sci.* **4,** 367–371
8. Ramalingam, S., Maxwell, S. E., Medof, M. E., Chen, R., Gerber, L. D., and Udenfriend, S. (1996) *Proc. Natl. Acad. Sci. U. S. A.* **93,** 7528–7533
9. Takeda, J., Miyata, T., Kawagoe, K., Iida, Y., Endo, Y., Fujita, T., Takahashi, M., Kitani, T., and Kinoshita, T. (1993) *Cell* **73,** 703–711
10. Inoue, N., Kinoshita, T., Orii, T., and Takeda, J. (1993) *J. Biol. Chem.* **268,** 6882–6885
11. Takahashi, M., Inoue, N., Ohishi, K., Maeda, Y., Nakamura, N., Endo, Y., Fujita, T., Takeda, J., and Kinoshita, T. (1996) *EMBO J.* **15,** 4254–4261
12. Miyata, T., Takeda, J., Iida, Y., Yamada, N., Inoue, N., Takahashi, M., Maeda, K., Kitani, T., and Kinoshita, T. (1993) *Science* **259,** 1318–1320
13. Kamitani, T., Chang, H. M., Rollins, C., Waneck, G. L., and Yeh, E. T. (1993) *J. Biol. Chem.* **268,** 20733–20736
14. Leidich, S. D., Kostova, Z., Latek, R. R., Costello, L. C., Drapp, D. A., Gray, W., Fassler, J. S., and Orlean, P. (1995) *J. Biol. Chem.* **270**, 13029–13035
15. Chen, R., Udenfriend, S., Prince, G. M., Maxwell, S. E., Ramalingam, S., Gerber, L. D., Knez, J., and Medof, M. E. (1996) *Proc. Natl. Acad. Sci. U. S. A.* **93,** 2280–2284
16. Leidich, S. D., and Orlean, P. (1996) *J. Biol. Chem.* **271,** 27829–27837
17. Leidich, S. D., Drapp, D. A., and Orlean, P. (1994) *J. Biol. Chem.* **269,** 10193–10196
18. Hamburger, D., Egerton, M., and Riezman, H. (1995) *J. Cell Biol.* **129,** 629–639
19. Benghezal, M., Benachour, A., Rusconi, S., Aebi, M., and Conzelmann, A. (1996) *EMBO J.* **15,** 6575–6583
20. Yu, J., Nagarajan, S., Knez, J. J., Udenfriend, S., Chen, R., and Medof, M. E. (1997) *Proc. Natl. Acad. Sci. U. S. A.* **94,** 12580–12585
21. Benghezal, M., Lipke, P. N., and Conzelmann, A. (1995) *J. Cell Biol.* **130,** 1333–1344
22. Canivenc-Gansel, E., Imhof, I., Reggiori, F., Burda, P., Conzelmann, A., and Benachour, A. (1998) *Glycobiology* **8,** 761–770
23. Sipos, G., Puoti, A., and Conzelmann, A. (1994) *EMBO J.* **13,** 2789–2796
24. Reggiori, F., Canivenc-Gansel, E., and Conzelmann, A. (1997) *EMBO J.* **16,** 3506–3518
25. Sanger, F., Nicklen, S., and Coulson, A. R. (1977) *Proc. Natl. Acad. Sci. U. S. A.* **74,** 5463–5467
26. Hill, J. E., Myers, A. M., Koerner, T. J., and Tzagoloff, A. (1993) *Yeast* **2,** 163–167
27. Gietz, R. D., and Sugino, A. (1988) *Gene* (*Amst.*) **74,** 527–534
28. Wach, A., Brachat, A., Pöhlmann, R., and Philippsen, P. (1994) *Yeast* **10,** 1793–1808
29. Harlow, E., and Lane, D. (1988) *Antibodies: A Laboratory Manual*, pp. 541–552, Cold Spring Harbor Laboratory, Cold Spring Harbor, NY
30. Feldheim, D., and Schekman, R. (1994) *J. Cell Biol.* **126,** 935–943
31. Baxter, B. K., James, P., Evans, T., and Craig, E. A. (1996) *Mol. Cell. Biol.* **16,** 6444–6456
32. Laemmli, U. K. (1970) *Nature* **227,** 680–685
33. Gaynor, E. C., and Emr, S. D. (1997) *J. Cell Biol.* **136,** 789–802
34. Puoti, A., Desponds, C., and Conzelmann, A. (1991) *J. Cell Biol.* **113,** 515–525
35. Ralton, J. E., Milne, K. G., Güther, M. L. S., Field, R. A., and Ferguson, M. A. J. (1993) *J. Biol. Chem.* **268,** 24183–24189
36. Roberts, W. L., Myher, J. J., Kuksis, A., Low, M. G., and Rosenberry, T. L. (1988) *J. Biol. Chem.* **263,** 18766–18775
37. Güther, M. L., Masterson, W. J., and Ferguson, M. A. (1994) *J. Biol. Chem.* **269,** 18694–18701
38. Puoti, A., and Conzelmann, A. (1992) *J. Biol. Chem.* **267,** 22673–22680
39. Puoti, A., and Conzelmann, A. (1993) *J. Biol. Chem.* **268,** 7215–7224
40. Schneider, P., Ferguson, M. A., McConville, M. J., Mehlert, A., Homans, S. W., and Bordier, C. (1990) *J. Biol. Chem.* **265,** 16955–16964
41. Sipos, G., Reggiori, F., Vionnet, C., and Conzelmann, A. (1997) *EMBO J.* **16,** 3494–3505
42. Ueda, E., Sevlever, D., Prince, G. M., Rosenberry, T. L., Hirose, S., and Medof, M. E. (1993) *J. Biol. Chem.* **268,** 9998–10002
43. Azzouz, N., Striepen, B., Gerold, P., Capdeville, Y., and Schwarz, R. T. (1995) *EMBO J.* **14,** 4422–4433
44. Deeg, M. A., Humphrey, D. R., Yang, S. H., Ferguson, T. R., Reinhold, V. N., and Rosenberry, T. L. (1992) *J. Biol. Chem.* **267,** 18573–18580
45. Treumann, A., Lifely, M. R., Schneider, P., and Ferguson, M. A. (1995) *J. Biol. Chem.* **270,** 6088–6099
46. Taguchi, R., Hamakawa, N., Harada Nishida, M., Fukui, T., Nojima, K., and Ikezawa, H. (1994) *Biochemistry* **33,** 1017–1022
47. Costello, L. C., and Orlean, P. (1992) *J. Biol. Chem.* **267,** 8599–8603

48. Carrington, D. M., Auffret, A., and Hanke, D. E. (1985) *Nature* **313,** 64–67
49. te Heesen, S., Rauhut, R., Aebersold, R., Abelson, J., and Aebi, M. (1991) *Eur. J. Cell Biol.* **56,** 8–18
50. Fankhauser, C., and Conzelmann, A. (1991) *Eur. J. Biochem.* **195,** 439–448
51. Franzusoff, A., Rothblatt, J., and Schekman, R. (1991) *Methods Enzymol.* **194,** 662–674
52. Conzelmann, A., Puoti, A., Lester, R. L., and Desponds, C. (1992) *EMBO J.* **11,** 457–466
53. Fankhauser, C., Homans, S. W., Thomas-Oates, J. E., McConville, M. J., Desponds, C., Conzelmann, A., and Ferguson, M. A. (1993) *J. Biol. Chem.* **268,** 26365–26374
54. Brewis, I. A., Ferguson, M. A., Mehlert, A., Turner, A. J., and Hooper, N. M. (1995) *J. Biol. Chem.* **270,** 22946–22956
55. Redman, C. A., Thomas Oates, J. E., Ogata, S., Ikehara, Y., and Ferguson, M. A. (1994) *Biochem. J.* **302,** 861–865
56. Homans, S. W., Ferguson, M. A., Dwek, R. A., Rademacher, T. W., Anand, R., and Williams, A. F. (1988) *Nature* **333,** 269–272
57. Stahl, N., Baldwin, M. A., Hecker, R., Pan, K.-M., Burlingame, A. L., and Prusiner, S. B. (1992) *Biochemistry* **31,** 5043–5053
58. Hirose, S., Prince, G. M., Sevlever, D., Ravi, L., Rosenberry, T. L., Ueda, E., and Medof, M. E. (1992) *J. Biol. Chem.* **267,** 16968–16974
59. Barlowe, C., Orci, L., Yeung, T., Hosobuchi, M., Hamamoto, S., Salama, N., Rexach, M. F., Ravazzola, M., Amherdt, M., and Schekman, R. (1994) *Cell* **77,** 895–907
60. Nelissen, B., De Wachter, R., and Goffeau, A. (1997) *FEMS Microbiol. Rev.* **21,** 113–134
61. Mondesert, G., Clark, D. J., and Reed, S. I. (1998) *Genetics* **147,** 421–434
62. Altschul, S. F., Madden, T. L., Schäffer, A. A., Zhang, J., Zhang, Z., Miller, W., and Lipman, D. J. (1997) *Nucleic Acids Res.* **25,** 3389–3402
63. Masterson, W. J., Doering, T. L., Hart, G. W., and Englund, P. T. (1989) *Cell* **56,** 793–800
64. Menon, A. K., Eppinger, M., Mayor, S., and Schwarz, R. T. (1993) *EMBO J.* **12,** 1907–1914
65. Nuoffer, C., Jeno, P., Conzelmann, A., and Riezman, H. (1991) *Mol. Cell. Biol.* **11,** 27–37

Deletion of *GPI7*, a Yeast Gene Required for Addition of a Side Chain to the Glycosylphosphatidylinositol (GPI) Core Structure, Affects GPI Protein Transport, Remodeling, and Cell Wall Integrity

Abdellah Benachour, György Sipos, Isabelle Flury, Fulvio Reggiori, Elisabeth Canivenc-Gansel, Christine Vionnet, Andreas Conzelmann and Mohammed Benghezal

J. Biol. Chem. 1999, 274:15251-15261.
doi: 10.1074/jbc.274.21.15251
